

# A Machine Learning Approach for Computer-Aided Detection of Cerebral Microbleed Using High-order Shape Features

Amir Fazlollahi<sup>1,2</sup>, Fabrice Meriaudeau<sup>2</sup>, Luca Giancardo<sup>3</sup>, Christopher C. Rowe<sup>4</sup>, Victor L. Villemagne<sup>4</sup>, Paul Yates<sup>4</sup>, Olivier Salvado<sup>1</sup>, Pierrick Bourgeat<sup>1</sup>, and on behalf of the AIBL Research Group<sup>5</sup>

<sup>1</sup>CSIRO Preventative Health Flagship, CSIRO Computational Informatics, Brisbane, QLD, Australia, <sup>2</sup>Le2i, University of Burgundy, Le Creusot, France, <sup>3</sup>RLE, Massachusetts Institute of Technology, MA, United States, <sup>4</sup>Department of Nuclear Medicine and Centre for PET, Austin Hospital, Melbourne, VIC, Australia, <sup>5</sup><http://www.aibl.csiro.au/>, Australia

**Introduction:** The incidence of cerebral microbleeds (CMBs) which are small spherical lesions containing iron has come to attention as a potential biomarker for cerebrovascular disease<sup>1</sup> and dementia<sup>2</sup>. MR susceptibility-weighted imaging (SWI) has shown superior sensitivity than conventional T2\*-GRE sequence for CMB detection, identifying more and smaller lesions. Visual rating, the current gold standard method for detecting CMBs, is time consuming, non-reproducible, subjective and prone to inter-reader variability as CMBs vary in size and contrast.

Several methods have been proposed for computer-aided detection of microbleeds using the Radial Symmetry Transform (RST)<sup>3,4</sup>, machine learning techniques<sup>5</sup> along with RST<sup>6</sup> or unified segmentation-normalization model<sup>7</sup>. All of these techniques suffer from low sensitivity, specificity and were mainly validated on small cohort sizes. The resulting performances (sensitivity, average false positives, total subjects) are (50%, NA, 30)<sup>7</sup>, (81.7%, 107, 6)<sup>5</sup>, (78%, 48, 72)<sup>4</sup>, (71.2%, 17.2, 18)<sup>3</sup>, (86.5%, 44.9, 15)<sup>6</sup> and (91%, 13.3, 30)<sup>8</sup> in our previous work.

This paper presents a novel machine learning approach for computer-aided detection of microbleeds in SWI. The major contributions are: identifying microbleed extent in order to extract proper cubic regions-of-interest (ROI) containing the structure, (2) extracting a set of robust 3-dimensional (3D) Radon- and Hessian-based shape descriptors within the ROIs as well as 2D Radon features computed on intensity-projection images of the corresponding ROIs, and (3) incorporating a cascade of random forests (RF) classifiers to iteratively reduce false detection rates while maintaining a high sensitivity.

**Method:** A subset of 66 participants with CMBs comprised of 11 subjects classified as Alzheimer's disease (AD), 14 as mild cognitive impairment (MCI) and 41 healthy controls (HC) from the Australian Imaging Biomarkers and Lifestyle (AIBL) study were included. For each subject, anatomical T1w and SWI MR images were available. All MRIs were acquired on a 3-T Siemens TRIO scanner. The 3D SWI used 0.9x0.9mm in-plane resolution and 1.75mm slice thickness, repetition time/echo time of 27/20msec, and flip angle 20°. Two clinical experts had inspected the SWIs using the MARS rating method<sup>9</sup> and in total 231 CMBs were found. 123 CMBs were labeled as "possible" and 108 as "definite".

The T1W images were segmented using an expectation maximization algorithm to generate skull-stripping masks and were then rigidly aligned to corresponding SWIs. The N4 bias field correction technique was performed to correct for intensity non-uniformity presents in SWIs. The dynamic intensity range of SWIs were then normalized to [0,1] after trimming the top 1% of intensities within the mask. To locally enhance the contrast and reduce noise, adaptive histogram equalization and gradient based anisotropic diffusion were carried out. The different processing steps of the proposed method are shown in Figure 1.

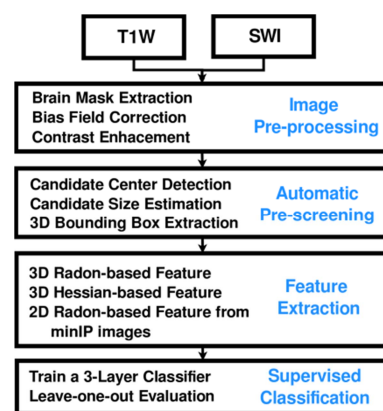


Figure 1. Overview of the proposed method

The aim in the screening phase is to identify and limit the analysis to potential regions containing CMB. We used a multi-scale spherical-like object detection approach for 3D brain images with a high sensitivity to small objects and a low false positive (FP) rate<sup>10</sup>. The multi-scale approach is capable of identifying the object extent along the x, y and z dimensions:  $\vec{R} = (r_x, r_y, r_z)$ . For each detected candidate, two patches with size  $1.5 \times \vec{R}$  and  $2.5 \times \vec{R}$  were considered. Within each patch, 3D Radon- and Hessian-based shape descriptors were computed: the mean ( $F_{\text{mean}}$ ) and standard deviation profiles ( $F_{\text{std}}$ ) computed across the Radon angle-dimension, standard deviation along the Radon angle-dimension ( $f_{\text{std}}$ ) and the global Radon mean ( $f_{\text{mean}}$ ). Using the eigenvalue decomposition of the Hessian matrix, the sphericalness ( $f_{\text{sphere}}$ ), largest cross-section ( $f_{\text{LC}}$ ), fractional anisotropy ( $f_{\text{FA}}$ ) and orientation ( $f_{\text{O}}$ ) were also computed. To address cross-sectional discontinuities due to anisotropic SWI acquisition, 2D Radon-based features were also computed over minimum-intensity projection (minIP) images of each major axis of ROIs. To achieve intensity shift invariance, the top and bottom 5% of the intensity values within the patches were removed and then rescaled to [0,1]. Radon descriptors are invariant to rotation and scale invariance is obtained by resizing the  $F_{\text{mean}}$  and  $F_{\text{std}}$  profiles to a fixed length. Translation invariance is enforced when the candidate microbleeds are placed at the center of the ROI prior to Radon transform. The Hessian features are rotation, scale and shift invariance. High sensitivity of the candidate selection step to irregular and low contrast microbleeds leads to an unbalanced training set with samples without distinct geometrical structure. In the current work, a 3-layer cascade of RF classifiers is proposed to address this issue. By increasing the RF probability threshold and adding FPs to the negative training examples of the following layer, the method can progressively build a balanced dataset without non informative candidates. A leave-one-out validation scheme was used to train the cascade which has a relatively balanced and informative training set in the final layer.

**Results:** For validation purposes, two subsets of "definite" (D) and "possible & definite" (PD) CMBs were formed. For D set an overall sensitivity of 94.4% and an average 7.61 false positives per subject were produced. The best performance for PD set had a sensitivity of 87% with an average false-positive rate of 20.2 per subject. The results are summarized in Table 1.

**Discussion:** In this work, a flexible machine learning framework is presented for detecting cerebral microbleeds on MR images. The proposed approach achieved higher performance and was validated on a larger number of subjects compare to previously published methods.

**References:** 1. Y. Nakata-Kudo *et al.* Dementia and geriatric cognitive disorders, 8-14, 2006, 2. P. Yates *et al.* *Neurology*, 77(1):48-54, 2011. 3. H.J. Kuijf *et al.* *NeuroImage*, 2011, 4. H. J. Kuijf *et al.* PLOS ONE, 8(6):e66610, 2013, 5. S.R.S. Barnes *et al.* *Magnetic Resonance Imaging*, 844-852, 2011, 6. W. Bian *et al.* *NeuroImage: Clinical*, Elsevier, 282-290, 2013, 7. M.L. Seghier *et al.* *PloS one*, 6(3):e17547, 2011, 8. A. Fazlollahi *et al.* ISMRM 2013, 9. S. Gregoire *et al.*, 2009, 73, 1759-1766, 10. A. Fazlollahi *et al.*, ICIP, 1158-1162, 2013,

Table 1. Evaluation of the proposed method on "definite" and "possible and definite" set

| Step        | Pre-screening |       | Overall results |       |
|-------------|---------------|-------|-----------------|-------|
|             | D             | PD    | D               | PD    |
| # TP        | 105           | 231   | 102             | 201   |
| Avg. FPs    | 668           | 1372  | 7.61            | 20.2  |
| # FN        | 3             | 8     | 6               | 30    |
| Sensitivity | 97.2%         | 96.5% | 94.4%           | 87.0% |